Scanning Electron Microscopy

Volume 1986 | Number 4 Article 2

9-11-1986

High Sensitivity Ion Microscopy: A Tool for Material Science Research

N. A. Thorne
Centre de Recherche

A. Dubus
Centre de Recherche

F. Degrève
Centre de Recherche

SCANNING ELECTRON MICROSCOPY/1986/IV (Pages 1255-1265)
SEM Inc., AMF O'Hare (Chicago), IL 60666-0507 USA

0586-5581/86$1.00+05

HIGH SENSITIVITY ION MICROSCOPY : A TOOL FOR MATERIAL SCIENCE RESEARCH

N.A. Thorne*, A. Dubus, F. Degrève

Cegedur Pechiney, Centre de Recherche,
38340 Voreppe, France

(Received for publication April 07, 1986, and in revised form September 11, 1986)

Abstract

Direct ion imaging is a strong point of the CAMECA IMS 3f ion microscope, but has undergone little commercial development. A modified image acquisition system is presented which incorporates a high sensitivity video camera allied with a rapid image digitizer/processor. Individual ion impacts on the channel plate are detected at maximum gain and image sensitivity is effectively increased to that of the mass spectrometer. For intermediate (10^3 to 10^5) and low (< 10^3) count rates image processing such as averaging or integration is essential to improve the poor detection statistics and allow real time image formation. Rapid image processing means that ion micrographs are immediately ready for interpretation or storage on a suitable medium. The improved instrument performance is illustrated from the point of view of materials science research: the routine use of an optimum lateral resolution, imaging at high mass resolution ($M/\Delta M$ = 20,000), improved imaging for insulating samples, trace element/molecular ion imaging and high quality images suitable for rapid transfer to an image analyzer for detailed quantitative analysis.

Key Words : Secondary Ion Mass Spectrometry (SIMS), high sensitivity ion microscopy, metallurgical SIMS, direct imaging SIMS, high mass resolution SIMS imaging, ion image analysis/processing.

*Address for correspondence:
For reprints and other information contact N.A. Thorne at the above address.
Phone no.: 76578000

Introduction

In the field of material science, Secondary Ion Mass Spectrometry (SIMS), with special emphasis on ion imaging, has proved to be a particularly well adapted research tool. The unique advantage of SIMS over other techniques lies in the detection of all elements in the periodic table with detection limits generally in the range of 1 to $10^{-3}\mu g/g$. The depth resolution of < 10nm for SIMS analysis is also of advantage as in certain cases the results may be considered as being two dimensional. A detailed review covering the use of SIMS for metallurgical applications may be found in the literature [5].

In the CAMECA IMS 3f ion microscope the sample surface is bombarded by a primary ion beam and the image formed by an electrostatic transfer lens system. After mass separation the ions constituting the image are projected onto a multi-channel plate/phosphor screen assembly for viewing[7]. This is in contrast to SIMS ion microprobes where the surface of the specimen is scanned by a finely focussed primary ion beam and resultant secondary ion images displayed on a synchronously scanned CRT. The IMS 3f secondary ion images are obtained virtually instantaneously, and are characterised by an optimum lateral resolution of better than 1μm.

To improve the performance of the image acquisition system of the IMS 3f three areas of development can be singled out, (1) reduction of the lateral resolution, (2) increase of the sensitivity in the imaging mode and (3) the provision of an interface with an image processor/analyzer. The only commercially available modification to the basic imaging system is that of Odom et al. [10], which uses a double channel plate to increase image sensitivity and a position sensitive Resistive Anode Encoder (R.A.E) to determine the position of arriving ions. The associated computer provides a digital image obtained directly from the position and number of detected ions. While this is an excellent system, flexibility is sacrificed due to the presence of a

maximum count rate of 10^5 cps beyond which the R.A.E is no longer position sensitive.

In the following we will present an alternative method[9], incorporating a high gain video camera and rapid image processing, which greatly improves the ion imaging performance of the CAMECA IMS 3f ion microscope. The wide range of areas in which improved or unique results have been obtained are illustrated using examples taken mainly from current materials science problems.

Experimental Procedure

In the IMS 3f the secondary ions constituting the image are projected onto a channel plate consisting of approximately 10^6 discrete electron multipliers or channels, each about 20μm in diameter. Approximately 60% of the arriving ions proceed to create within individual channels about 10^3 electrons each which are subsequently accelerated onto a phosphor screen where the image is viewed with a Vidicon type video camera.

The modified image acquisition system that we have adopted is presented schematically in Figure 1. Two improvements have been made to the basic IMS 3f system. The phosphor screen is now viewed with a high gain, low light level video camera and the resultant images passed through an image processor. The add-on nature of the above system ensures that no mechanical or electrical alteration to the basic IMS 3f is required.

Low Light Level Camera

Vidicon cameras are generally capable of producing images with target illuminations of 0.1 Lux while Nocticon cameras, more commonly employed on Transmission Electron Microscopes, guarantee images with illuminations as low as 10^{-4} Lux. Compared to the basic IMS 3F an improvement in image sensitivity of between 10^2 and 10^3 has thus been achieved by simply substituting a low light level Nocticon type camera (LHESA electronique, 95310 Saint-Ouen-L'Aumone, France). The camera construction includes a fibre optic/photocathode faceplate onto which the image from the phosphor screen is projected, followed by an image intensifier which accelerates the photoelectrons onto an electron multiplying target. Every 1/25s a scanning electron beam "reads" the target to form the image which is subsequently output in analogue form. The gain of the intensifier may be manually or automatically controlled, the automatic gain control providing a safety feature preventing accidental over-saturation and damage to the target. The variable gain ensures that image formation is possible over the entire range of count rates encountered with this instrument (<10 to10^8 cps), as at maximum gain individual secondary ions arriving at the channel plate are visually detected.

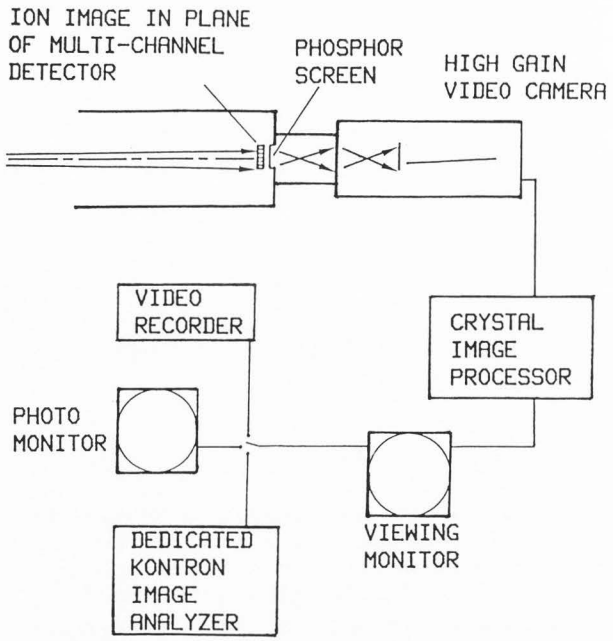

Figure1: Schematic diagram of the modified IMS 3f image acquisition system including a high sensitivity video camera, high speed image digitization / processing and options for image recording or further image analysis.

The only barrier preventing real time image formation is the poor detection statistics associated with count rates <10^5. For this reason the full advantages of high sensitivity image detection may only be fully appreciated in association with rapid image processing.

Image Processing

Incoming images arriving from the camera at the rate of 25 frames per second are digitized to a depth of 8 bits (256 grey levels) for subsequent image processing (Quantel Micro consultants "CRYSTAL", 78000 Versailles, France). The choice of image processing performed depends primarily on the secondary ion count rate:

Straight through imaging (i.e. >10^5cps) : No image processing is performed , the output signal is the real time image output by the camera.

Image averaging : To improve the detection statistics for count rates between 10^3 to 10^5 cps the image output by the processor is the average of n frames. For small n a floating average mode is available which improves image quality while being transparent to the operator.

Integration : The integrated signal from n frames (continuously displayed during acquisition) provides a method of obtaining images with as little as 10 to 10^3 cps. Integration times depend on the depth resolution required, the count rates available and the lateral distribution of the element concerned.

Image storage : Two framestores are available in the basic system to allow a reference image to be recalled for comparison.

The optimized image resulting from the above operations is ready for immediate interpretation and may be photographed, recorded on magnetic tape for deferred viewing or transferred to a dedicated image analyzer (Kontron, SEM IPS, Kontron Bild Analyse, D-8057 Munich, Germany) for further processing.

Typically, the image analyzer is used for image manipulations such as normalization with a reference image, image superposition, determination of the number, size or surface fraction of a given feature within an image, or quantification of images where the pixel grey levels are proportional to element concentration.

Background Noise

With the ion pump at the exit of the mass spectrometer switched off, the image acquisition system at maximum sensitivity is characterised by zero background signal. With the secondary ion extraction field at zero and hence no secondary ions characteristic of the sample reaching the channel plate, image integration for several minutes results in a blank screen. This is considered indispensible and means that each image feature corresponds to the detection of a secondary ion of the selected mass.

Results and Discussion

Modes of Image Processing

The image processor is present in order to allow imaging in real time when the detection statistics are poor. The two operating modes generally used are illustrated below.

Image averaging (10^3 to 10^5 cps) : With count rates of the order of 10^3 to 10^5 cps the poor detection statistics result in images having a "noisy", fluctuating appearance. The light emitted at a given point on the phosphor screen due to a detected ion has time to fall to zero before the detection of another ion at the same point. Immediate interpretation of the image is not always possible and fine detail may be lost to the operator. The ability to average n frames allows a real time improvement of the detection statistics and replaces "blind" exposures using a standard 35 mm camera.

The comparison between real time and averaged images is illustrated in Figure 2 for a copper free aluminium alloy used as a cladding on a copper containing alloy, the whole having been heat treated. Figures 2a and 2b illustrate respectively the real time $^{63}Cu^+$ and $^{27}Al^+$ images obtained during argon bombardment with 10^3 and 10^5 cps respectively. Oxygen flooding was used for the Cu image but not for the Al image, the resultant crystallographic contrast revealing the presence of the aluminium grain boundaries. Figures 2c and 2d present the improved images resulting from averaging 450 frames (18s) for $^{63}Cu^+$ and 125 frames (5s) for $^{27}Al^+$. It can be seen that during the particular heat treatment applied the copper of the underlying copper containing alloy diffused through the cladding material by way of the grain boundaries.

Image integration (<10^3cps) : The high speed integration mode combined with individual ion detection means that the image sensitivity of the IMS 3f is effectively increased to that of its double focussing mass spectrometer. A simple example can be given using a standard copper grid deposited on aluminium, where 500 cps were noticed for $^7Li^+$. Figure 3a shows the $^{27}Al^+$ image and Figure 3b the real time $^7Li^+$ image as seen by the operator. No interpretation concerning the lateral distribution of Li is possible. Figure 3c illustrates the result of integrating 175 frames (7s) under exactly the same bombardment conditions. Lithium is clearly present at the interface between the aluminium and copper.

It is worth comparing the above operating mode with that of a SIMS ion microprobe [11]. While the sensitivity of the two instrument types may be similar, image acquisition times vary enormously. In the case of a microprobe, the lower the count rate the longer the dwell time (integration time) at each image point or pixel. For example, a 5 ms dwell time will require 20 minutes to obtain a 512 x 512 pixel image. However, with a count rate of, say, 1000 cps, a 5 ms dwell time will result in only 5 counts at each pixel. In contrast, an ion microscope integrates the whole image simultaneously and in 20 minutes would accumulate 1.2×10^6 counts at each pixel.

Improved Instrument Performance

The improved ion imaging means that the ion microscope can now be used under operating conditions which optimize its performance (e.g., lateral resolution), but which would normally inhibit image formation due to a reduced secondary ion signal. In addition, materials science problems not normally considered, or at best extremely difficult with SIMS, may now be undertaken:

a) trace element analysis. All peaks present in a mass spectrum may be investigated in the image mode.
b) lateral distribution of elements within thin surface films where virtually static SIMS is required.
c) imaging of molecular ions, at low or high mass resolution, providing chemical information (e.g., intermetallic phase or organic material identification).
d) irradiation sensitive or insulating materials where low flux density ion or neutral beams are desirable [3][2].

The above topics are used to illustrate the improved IMS 3f performance. Unless otherwise stated the samples were bombarded by an argon ion beam (8keV) in the presence of oxygen flooding.

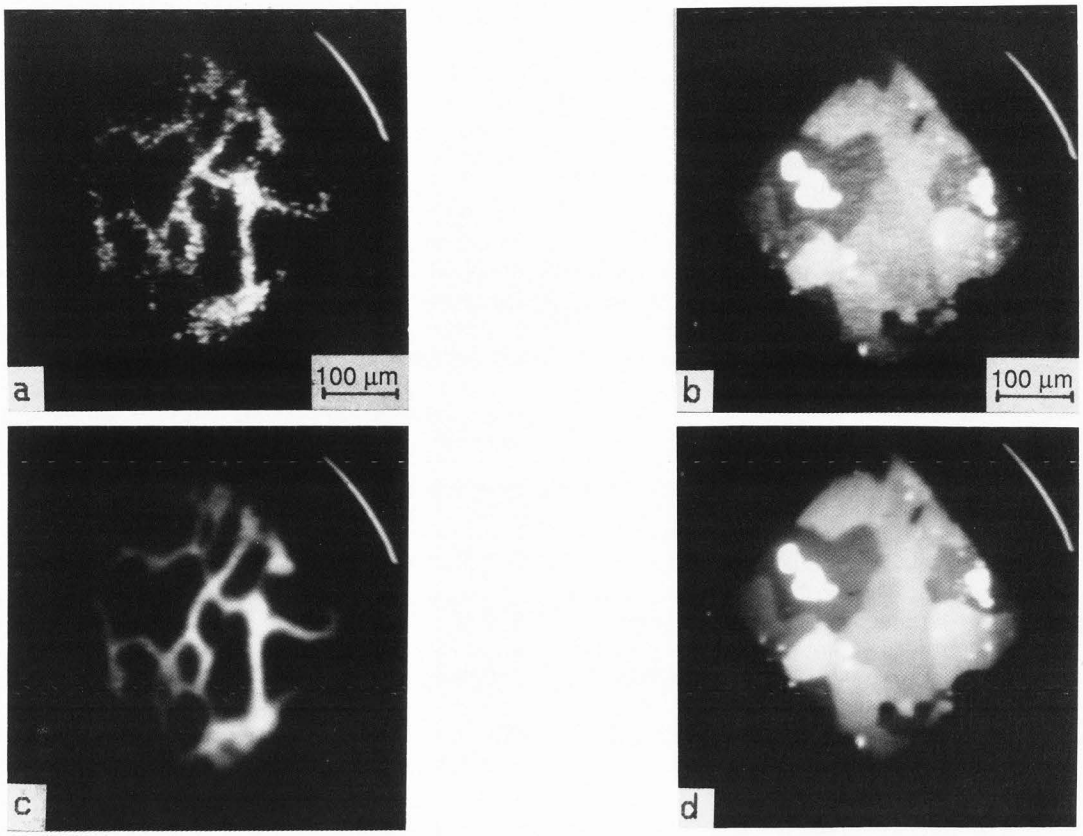

Figure 2: High speed image averaging improves the detection statistics and hence image quality. The example shows grain boundary copper diffusion through a copper free aluminium alloy.
a) $^{63}Cu^+$ and b) $^{27}Al^+$ real time ion micrographs, c) $^{63}Cu^+$ averaged for 450 frames (18s) and d) $^{27}Al^+$ averaged for 125 frames (5s).

These conditions are generally preferred as they provide flexibility (e.g., crystallographic contrast can be rapidly obtained by stopping the oxygen flooding), while ensuring adequate surface oxygen coverage[8] for optimized count rates and reduced matrix effects. Recent work[1] suggests that the subsequent lateral resolution of the ion images may be reduced due to the increased pressure in the specimen chamber. However, it is considered of secondary importance compared to the rôle played by the channel plate detection system, as discussed below.

Lateral resolution : Depending on the operating conditions the optimum lateral resolution of ion micrographs may be limited by either the ion optics or the detection system. The major source of image astigmatism is the presence of ions emitted from the sample with a high angle and energy component. For the ion optics to achieve a lateral resolution of better than 1µm these ions must be eliminated[11]. This is achieved by placing a diaphragm (D_C) at the cross-over in the transfer lens configuration and by using the energy filter of the spectrometer. The diameter of D_C depends on which of the three pre-set image fields is selected, and must be less than 150, 60 and 12µm for imaged fields of 400, 150 and 25µm respectively. Evidently, for a given imaged field the smaller the D_C the lower the count rate and a compromise is often sought between lateral resolution and sensitivity. The modified system allows the routine use of a theoretical lateral resolution, even for trace elements, of better than 1µm.

In reality the lateral resolution is often limited by the detection system. For example, when viewing a field of 150µm the image is projected onto an area of about 500 x 500 channels, each channel thus representing about 0.3µm in diameter. However, on leaving the channel plate the electrons spread out and the phosphor screen emits light over a larger area, corresponding to approximately 1.5µm in the image. Under these conditions it is the electron spreading which ultimately limits the lateral resolution. This is seen in Figure 4 with the $^{56}Fe^+$ image from a standard aluminium sample containing 155µg/g of Fe uniformly distributed in the solid solution. The count rate during image integration (125s) was only 300 cps. The lateral resolution is determined by the "impact" diameters. Image magnification with the projection lenses may reduce the effective "ion impact" diameter to around 0.5µm,

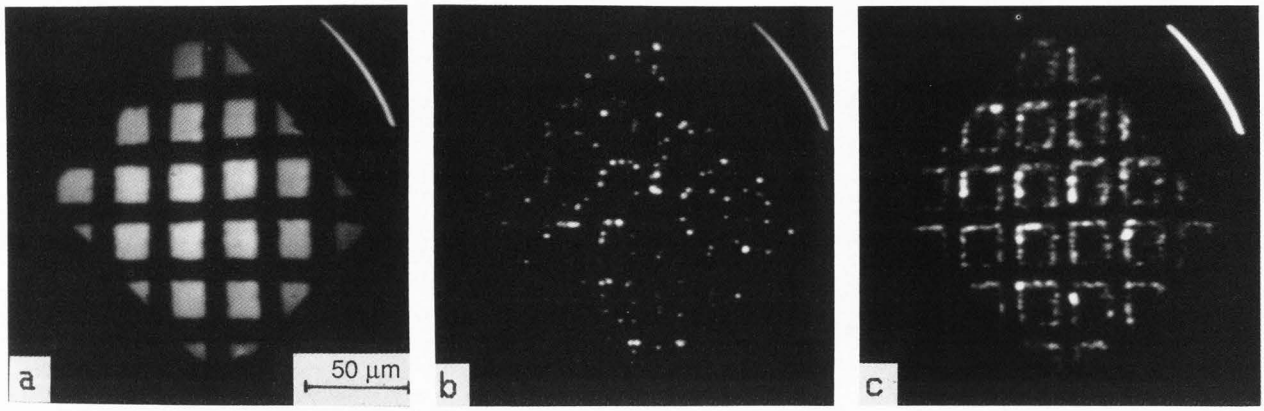

Figure 3: Image integration allows imaging with count rates < 10^3 cps.
a) $^{27}Al^+$ ion micrograph of a standard copper grid deposited on an aluminium substrate
b) $^{7}Li^+$ real time image (500 cps)
c) $^{7}Li^+$ image after integrating 175 frames (7s).

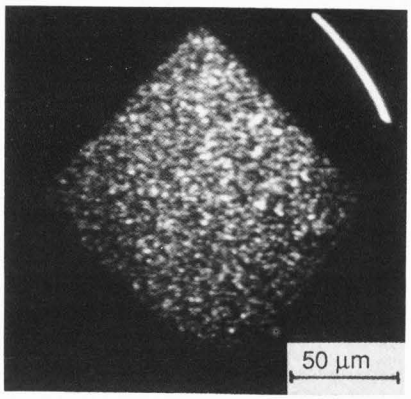

Figure 4: $^{56}Fe^+$ micrograph of an aluminium sample containing 155µg/g of iron in the solid solution. Each white spot represents the detection of a secondary $^{56}Fe^+$ ion. Image resolution is limited by the diameter of the impacts (integrated image of 3,132 frames).

but simultaneously reduces the secondary ion flux density by a factor of 10.

Image magnification is best achieved by selecting an imaged field of 25µm, where the increased acceptance angle compensates to keep the sensitivity high. Under these conditions an ion impact represents only 0.2µm in the image and the projector lenses allow a further reduction to < 0.1µm. As stated above a 25µm field requires a D_C of < 12µm to achieve a lateral resolution of better than 1µm. Figure 5 presents a typical result using a D_C of 5µm in diameter (20µm is the smallest normally provided). The sample is an Al/Fe binary alloy with fine interdendritic Fe rich phases. The apparent thickness of the intermetallic phases seen in the $^{56}Fe^+$ ion micrograph suggests a lateral resolution of at least 0.4µm.

Quantitative micro-analysis : In certain cases a good lateral resolution with low available count rates is a prerequisite for quantitative micro-analysis. A typical case may be illustrated using the same Al/Fe binary alloy as above. The determination of the Fe concentration in the solid solution requires an analysis which excludes the finely dispersed Fe rich phases. All previous attempts at obtaining ion images which correctly resolved the solid solution failed as the $^{56}Fe^+$ signal is very low. The $^{27}Al^+$ signal from the solid solution and from the phases cannot be used as a reference image due to a lack of contrast.

Figure 6 presents an $^{56}Fe^+$ ion micrograph and a lateral $^{56}Fe^+$ "step-scan" obtained in the same region by displacing a zone of 1µm diameter in steps of 1µm. The step-scan suggests an Fe content which declines towards the center of the dendrites and reaches minima at 350 and 470µg/g. It is interesting to note that each analysis point involved a sample of 10^{-14}g of aluminium and hence only 4 x 10^{-18}g of iron (about 43,000 atoms). The two dimensional quality of SIMS is indispensable in the above example, where the proximity of underlying Fe rich phases cannot be neglected when using more conventional techniques (EPMA)[5].

Insulating samples : The IMS 3f of our laboratory is equipped with a Fast Atom Beam (FAB) source enabling the analysis of insulating or irradiation sensitive materials[3][2]. The details of the source are fully given elsewhere[4]. Briefly, a gas collision chamber has been inserted in the primary column yielding a neutral beam of significant intensity. The remaining primary ions are deflected away from the sample. Positive and negative mass spectra and ion imaging (Fast Atom Beam Ion Microscopy or FABIM) are possible. Secondary negative ion imaging is the most problematic as the sample surface potential increases by about 100eV. For secondary positive ions the surface potential rests virtually unchanged and imaging is only "hindered" by lower count rates than encountered under ion bombardment. Image averaging and integration allow ion imaging of insulating samples with an optimum lateral resolution.

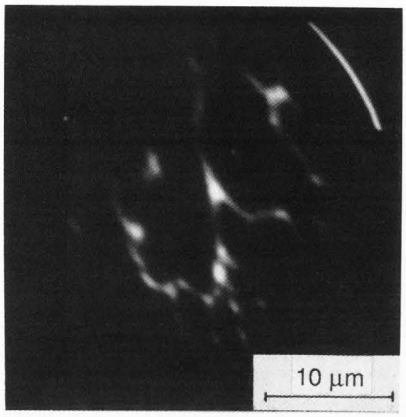

Figure 5: The optimum lateral resolution of the ion images is obtained using an imaged field of 25µm and a contrast diaphragm D_c of 5µm. A lateral resolution of ≤ 0.4µm may be estimated from the $^{56}Fe^+$ image obtained from an Al/Fe binary alloy (obtained by averaging for 45s).

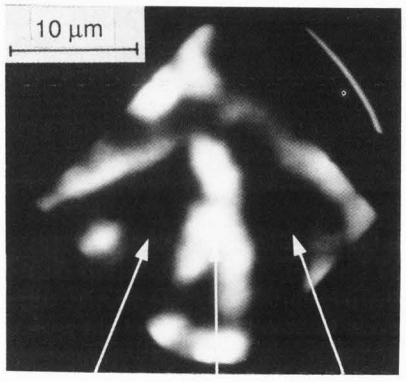

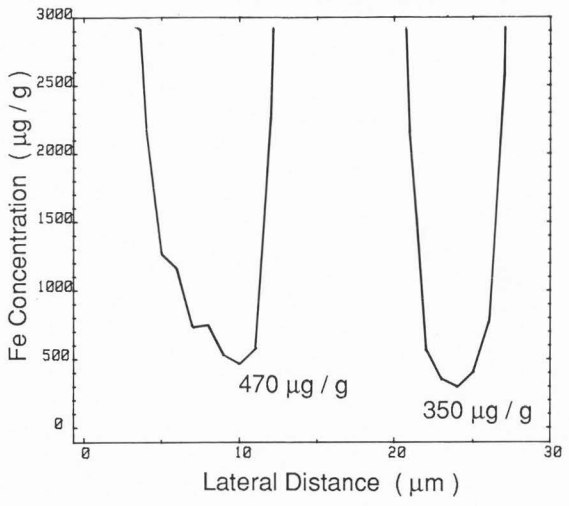

Figure 6: Quantitative micro-analysis of Fe in the solid solution of the Al/Fe alloy of Figure 5. The $^{56}Fe^+$ image and lateral scan of the same zone show a minimum iron concentration at the center of the dendrites (350 to 470µg/g).

Figures 7a and 7b present the $^{40}Ca^+$ and $^{24}Mg^+$ ion micrographs obtained from an insulating sample under Ar° bombardment. The sample was taken from the accumulated deposits at the base of a beer vat and contains essentially calcium and magnesium. The lateral resolution of the image may be seen from comparing the detail in the two images. No secondary ion signal could be obtained when the specimen was bombarded by a primary ion source.

Molecular ions/surface films : The determination of the elemental distribution within thin surface films is greatly facilitated by the image integration mode. The following example concerns an aluminium sample having an average of only a few monolayers of a silane molecule deposited on its surface. In adhesive bonding silane increases the bond strength by acting as a bridge between the surface oxide and subsequently deposited adhesives or polymer films. After obtaining mass spectra under Ar^+ (2.5 keV) bombardment with a total dose of 10^{12} ions/cm^2 it was found that the $^{45}SiOH^+$ molecule could be used as characteristic of the silane molecule (no oxygen flooding was used). Molecular ion micrographs were obtained using a current density of 10^{15} ions/cm^2.s and integration meant a total dose of 5×10^{16} ions/cm^2.

Figure 8a shows the $^{27}Al^+$ image revealing areas of the aluminium surface oxide. The dark regions correspond to the silane surface distribution as seen by the $^{45}SiOH^+$ ion micrograph of Figure 8b. For the particular application process employed the silane was non-uniformly distributed at the micron scale. The use of a primary neutral beam may well minimize irradiation damage of such organic coatings and further improve the possibilities of molecular ion imaging.

Molecular ions are commonly present as interference peaks requiring high mass resolution to separate them from other peaks in the spectrum. An example of molecular ion imaging at a mass resolution of up to 20,000 is presented in the following section.

Ion imaging at high mass resolution : The mass resolving power of the IMS 3f instrument is variable from $M/\Delta M = 300$ to about 10,000 in the spectrometric mode, i.e. magnetic field scanning, or double this in the "static imaging" or spectrographic mode. When it comes to the interpretation of the complicated spectra observed with heterogeneous, multi-element metallurgical samples this is an indispensable aid. Imaging at high mass resolution allows the easy separation of interference peaks, particularly useful when alternative isotopes etc. cannot be used, as well as providing a means of determining the surface distribution of molecular ions to obtain unique chemical information. However, the mass resolution is inversely proportional to the spectrometer entry slit width and hence high mass resolution means lower

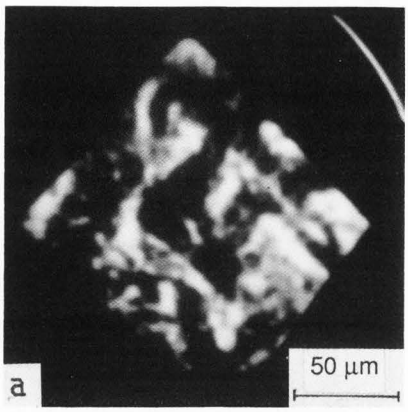

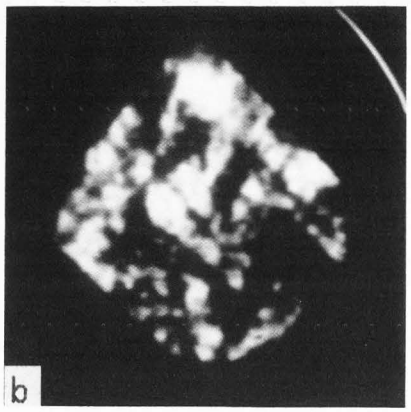

Figure 7: $^{40}Ca^+$ (a) and $^{24}Mg^+$ (b) ion micrographs obtained under Ar^+ bombardment of an insulating sample (FABIM). The detail within the images illustrates the lateral resolution of about 1.5μm.

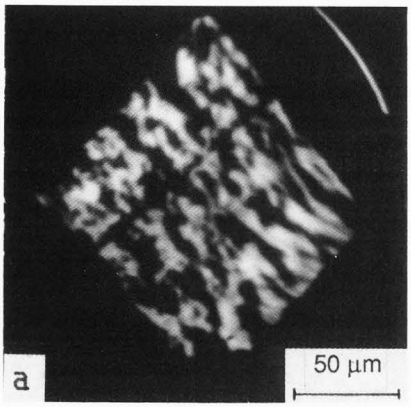

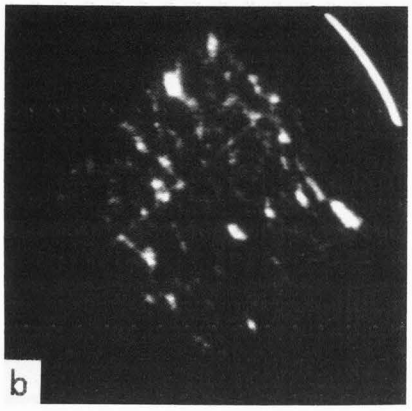

Figure 8: Ion imaging within thin surface films is illustrated by an aluminium sample covered with a several monolayer thick silane layer. The substrate is revealed by the $^{27}Al^+$ image (a) and the $^{45}SiOH^+$ molecular ion image (b), obtained by integrating for 55s, confirms the heterogeneous silane distribution.

sensitivity. For this reason ion imaging at high mass resolution is not normally considered.

The operating conditions used to obtain mass spectra optimize both the sensitivity and mass resolution. Ion images obtained under these conditions are distorted and are of poor lateral resolution (large D_c at the cross-over). For ion microscopy at high mass resolution the entry slits may be left open, as a small D_c at the cross-over provides good lateral resolution images as well as improving the mass resolution by reducing the effective width of the entry slits. However, the diaphragm also reduces the effective slit height with a subsequent reduction in count rate. Image integration may be used to recuperate ion images when the available count rates are very low.

With the spectrometer slits open and using a D_c of 20μm, mass spectra may be obtained with $M/\Delta M$ = 4,000 by sufficiently reducing the pass band of the energy filter and by reducing the imaged field to around 60μm. Figure 9a illustrates a direct imaging mass spectrum at the nominal mass of 56 Daltons using a D_c of 20μm. The two "peaks" correspond to $^{56}Fe^+$ (55.9349) and $^{28}Si_2^+$ (55.9539). The mass resolution in this spectrographic mode is of the order of 8000. The sample consisted of a composite material of SiC particles in an Al matrix. Figures 9b, 9c and 9d show the $^{56}Fe^+$, $^{28}Si_2^+$ and $^{27}Al^+$ micrographs respectively, obtained under identical operating conditions. The Fe is shown to be non-uniform, probably due to Fe rich intermetallics precipitated at the matrix/particle interface.

By using a D_c of only 5μm in diameter the mass resolution should, assuming that the spectrometer aberrations do not dominate, extend up to 16,000 for mass spectra. In practice, a mass resolution of 13,500 has been obtained, as illustrated in Figure 10 by the mass spectrum at the mass 28 for a silicon wafer. For the same operating conditions Figure 11a illustrates a direct imaging mass spectrum of the mass 31 obtained on an Al/Li alloy. The three peaks visible are, from left to right, $^{24}Mg^7Li^+$ (31.0010) with a probable contribution from $^{25}Mg^6Li^+$ (31.0009), $^7Li_2{}^{17}O^+$ (31.0311) and $^7Li_2{}^{16}O^1H^+$ (31.0348).

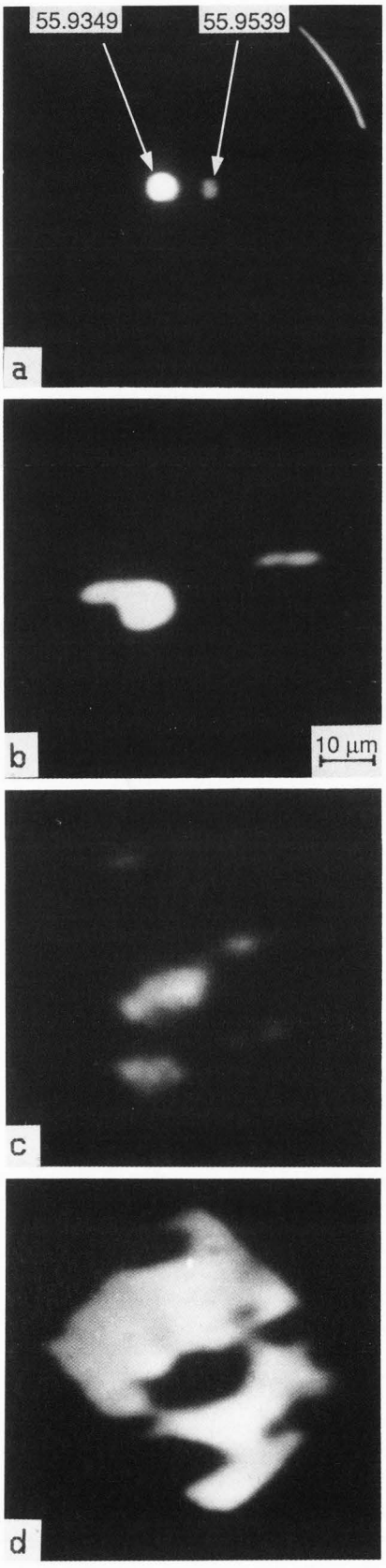

Figure 9: Ion imaging with a mass resolution M/ΔM=8,000 illustrated for a composite material (Al/SiC).

a) mass spectrography; direct imaging mass spectrum at the mass 56 with $^{56}Fe^+$ (55.9349) on the left and $^{28}Si_2^+$ (55.9539) on the right.

b) $^{56}Fe^+$ image.

c) $^{28}Si_2^+$ image.

d) $^{27}Al^+$ image.

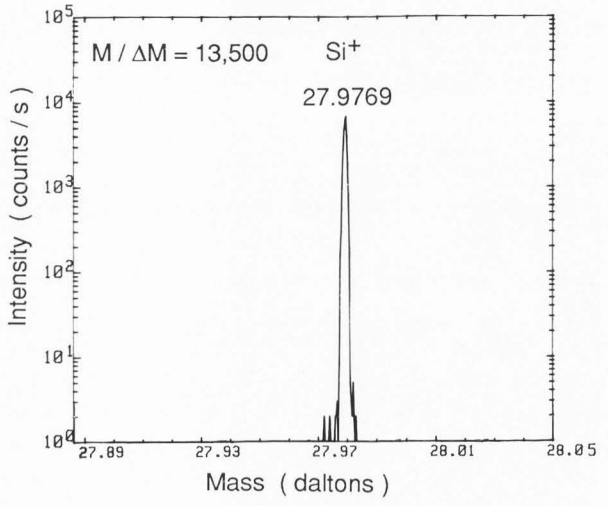

Figure 10: Mass spectrum obtained at the mass 28 on a Si wafer. A contrast diaphragm D_c of 5µm was used to obtain a mass resolution M/ΔM of 13,500.

The two extreme peaks thus differ by 0.0338 Daltons and the mass resolution is ≤ 20,000. Figure 11b shows the ion micrograph of the molecular ion(s) $^{24}Mg^7Li^+/^{25}Mg^6Li^+$ obtained under the same conditions of mass resolution, the peak representing only 200cps. The magnesium and lithium containing intermetallic phases are clearly identified. To illustrate the quality of the high mass resolution image, Figure 11c presents a low mass resolution $^7Li^+$ image of the same zone. It can be seen that at high mass resolution image distortion is limited to a slight flattening.

Quantitative image analysis : Under certain sampling conditions all or part of an ion image may be considered as quantitatively representing the two-dimensional distribution of an element and quantitative image analysis may be considered. To eliminate spurious effects such as non-uniform channel plate or camera response, the image of the element of interest is first normalized with respect to the image of the matrix element ($Image_x/Image_{mat.}$).

After initial image processing (averaging) to improve the detection statistics the two images are transferred to the image analyzer. Each pixel of $image_x$ is divided by the corresponding pixel of

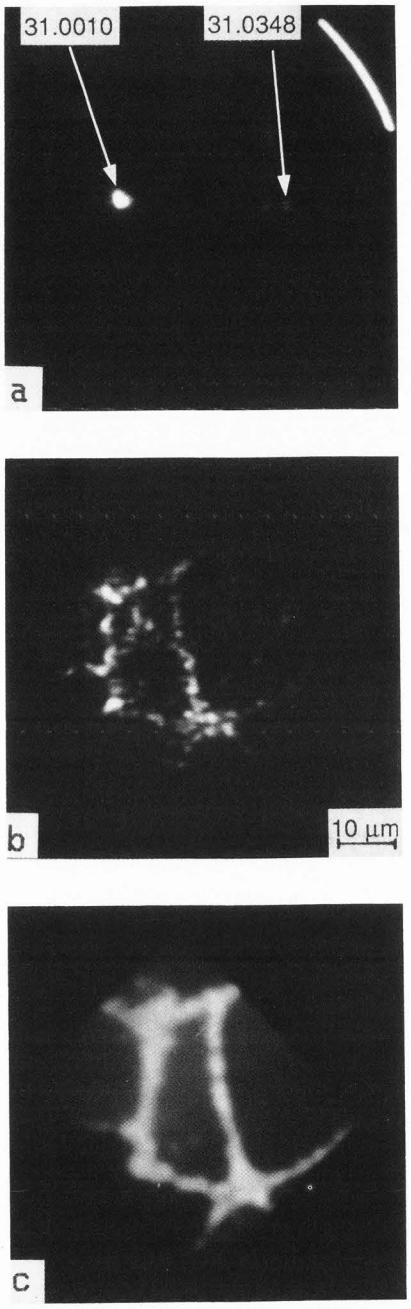

Figure 11: Molecular ion imaging with the mass resolution of Figure 10.

a) Direct imaging mass spectrum of the mass 31 for an Al/Li alloy with, from left to right, $^{24}Mg^{7}Li^{+}$ / $^{25}Mg^{6}Li^{+}$ (31.0010), $^{7}Li_{2}{}^{17}O^{+}$ (31.0311) and $^{7}Li_{2}{}^{16}O^{1}H^{+}$ (31.0348).

b) ion image of the molecular ion $^{24}Mg^{7}Li^{+}$ / $^{25}Mg^{6}Li^{+}$.

c) $^{7}Li^{+}$ image of the same zone obtained at low mass resolution.

$image_{mat.}$ to obtain the normalized image[6]. If required the limited number of point defects arising from the camera target may be eliminated by a suitable algorithm prior to normalization. As long as matrix effects do not occur or are taken into account (e.g., by masking all but the region of interest), each pixel grey level is now proportional to the concentration of the element of interest. The normalized image may be used in conjunction with suitable standards to obtain rapidly and accurately the quantitative lateral distribution of the element in any chosen direction, or to obtain the concentration histogram in any selected zone.

To illustrate the approach, Figure 12 presents the comparison of three techniques used to obtain the magnesium concentration gradient in the as-cast microstructure of an aluminium/lithium alloy. The three curves were obtained by performing lateral scans of the same grain using :

1) Electron Probe Micro Analysis (curve a).

2) SIMS lateral scan obtained by displacing the specimen laterally with respect to the defined analysis zone (curve b).

3) a lateral pixel analysis from a normalized $^{24}Mg^{+}$ image (curve c).

The three scans are identical within reasonable experimental error. Grain boundary magnesium containing intermetallic phases were incorporated in the line scans (b,c) and represent regions where matrix effects rule out their use with the chosen standards. Within these regions the concentration scale for curves b and c are no longer valid. Note that with a lateral SIMS scan the lateral resolution of about 2-3µm is defined by the diameter of the analysis zone chosen, while for image analysis the

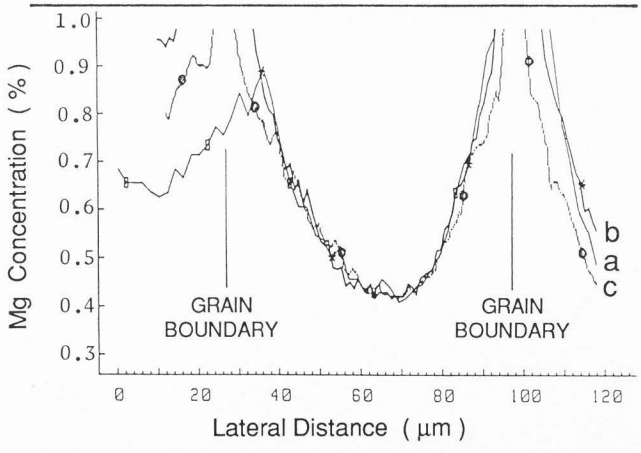

Figure 12: Comparison of quantitative lateral scans of the Mg concentration within an as-cast Al/Li alloy using 3 different techniques:

a) EPMA.

b) SIMS lateral "step-scan".

c) Lateral pixel scan obtained from a normalized SIMS ion micrograph.

lateral resolution is that of the image (in the present case about 1.5μm). For this reason the intergranular magnesium rich intermetallics are better resolved and appear narrower in the case of curve c.

Figure 13 presents the normalized $^{24}Mg^+$ ion micrograph of the same zone used to obtain the curves above. In this case the magnesium concentration gradient is visually illustrated by adding false colours corresponding to concentration steps of 0.5 %. It must be emphasized that due to matrix effects the grain boundary intermetallic phases (white) do not correspond to the concentration scale shown. Quantitative analysis of the solid solution (e.g., concentration histograms), requires the removal of such regions by the image analyzer using standard masking routines.

Conclusions

The use of a low light level high sensitivity camera, combined with an image processor, greatly improves the ion imaging capabilities of the CAMECA IMS 3f ion microscope. A gain of up to 10^3 in image sensitivity allows the visual detection of individual secondary ions. This means that ion imaging is possible for all peaks present in mass spectra with count rates ranging from <10 to over 10^8 cps. For intermediate and low count rates where the detection statistics are poor, image processing (averaging or integration) allows the acquisition of good quality images which are ready for immediate interpretation or further image analysis. Virtually all operating modes of the IMS 3f are improved. Consequently, ion microscopy may be performed with the routine use of an optimum lateral resolution, at high mass resolution, under near static SIMS conditions or, in the presence of a FAB source, on insulating or irradiation sensitive samples.

Acknowledgments

The authors wish to thank Mrs. Dussouillez, Mrs. Madelan and Mrs. Terroni for their technical assistance.

References

1) Bernius M. T, Ling Y. C, Morrison G. H. (1986). Evaluation of Ion Microscopic Spatial Resolution and Image Quality. Anal.Chem. 58, 94.

2) Briggs D, Hearn M. J. (1985). Analysis and Chemical Imaging of Polymer Surfaces by Secondary Ion Mass Spectrometry. Spectrochemica Acta, 40B, N° 5/6, 707-715.

3) Brown A, Van Den Berg J. A, Vickerman J. C. (1985). A Comparison of Atom and Ion Induced SIMS. Evidence for Charge Induced Damage Effects in Insulator Materials. Spectrochemica Acta, 40B, N° 5/6, 871-877.

4) Degrève F, Lang J. M. (1985). Use of a Fast Atom Beam in Ion Microscopy (FABIM) for Analysis of Poorly Conducting Materials. Surf. Interface Anal. 7, 177-187.

5) Degrève F, Lang J. M. (1986). Metallurgical Applications of SIMS, in: Secondary Ion Mass Spectrometry, SIMS V, Springer Verlag, Berlin, 388-393.

6) Fassett J. D, Morrison G. H. (1978). Digital Image Processing in Ion Microscopic Analysis: Study of Crystal Structure Effects in Secondary Ion Mass Spectrometry. Anal. Chem. 50, 1861-1866.

7) Gourgout J. M. (1979). Use of the IMS 3f High Mass Resolving Power, in: Secondary Ion Mass Spectrometry, SIMS II, Springer Verlag, Berlin, 286- 290.

8) Lang J. M, Degrève F. (1985). Oxygen Coverage Effects in SIMS Quantitative Analysis Using a Primary Rastered Probe. Surf. Interface Anal. 7, 53-61.

9) Leta D. P. (1986). A High Resolution, Single Ion Sensitivity Video System for Secondary Ion Microscopy, in: Secondary Ion Mass Spectrometry, SIMS V, Springer Verlag, Berlin, 232-234.

10) Odom R. W, Furman B. K, Evans Jr. C. A, Bryson C. E, Peterson W. A, Kelly M. A, Wayne D. H. (1983). Quantitative Image Acquisition System for Ion Microscopy Based on the Resistive Anode Encoder. Anal. Chem. 55, 574-578.

11) Slodzian G. (1980). Microanalyzers Using Secondary Ion Emission, in: Applied Charged Particle Optics, Adv. in Electronics and Electron Physics, Suppl. 13B, A. Septier, Academic Press, N.Y. 1-44.

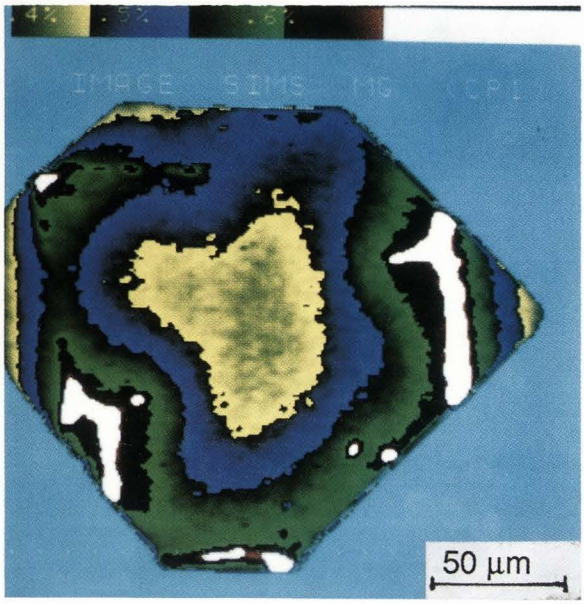

Figure 13: The normalized secondary ion image ($^{24}Mg^{+}/^{27}Al^{+}$) used to obtain curve c of Figure 12, but after image quantification. The colour scale corresponding to Mg concentration steps of 0.5% is given at the top of the figure.

Discussion with Reviewers

W. Katz : You state that the use of neutral bombardment may reduce irradiation damage in organics - could you explain why this might be?
Authors : We rarely deal with bulk organic materials where the effects of extended irradiation by ion or neutral beams can be observed. At present we more commonly study thin surface films or deposits which are rapidly sputtered away. We have based our comment on the results of Brown et al. [3] where it is suggested that the dissipation of charge introduced by an ion beam contributes to the damage mechanism.

W. Katz : Do you have any idea how much the image quality degrades, particularly in metallurgical systems prone to grain boundary types of sputtering, as a function of image integration time?
Authors : We have not tried to quantify image degradation. For all but trace element analysis image integration/averaging routines rarely represent the erosion of more than about 100 Å and no degradation is observed. For integration times of several minutes or more however the major problem encountered is the creation of a "step" between regions of different sputtering rate (eg., between grains, intermetallic phases, regions of different composition, etc.). The result can be the superposition of a topographical contrast and a chemical contrast.

A. Lodding : The great value of the modification you describe appears to lie in the much improved detection sensitivity in the image mode. Could you quote actual figures comparing the sensitivity of your system to that of the present Cameca standard image stage?
Authors : The increased image sensitivity of our modified system comes entirely from the difference in video camera performance used to view the phosphor screen (as each arriving ion emits a finite quantity of light at the phosphor screen). The Nocticon type camera used by ourselves is approximately 1000 times more sensitive than the Vidicon type camera installed as standard. The resultant sensitivity is similar to that obtained using a double channel plate, but in our case the additional intensifier is outside the instrument and thus entails no modifications.

A. Lodding : You qoute zero background signal "with the ion pump at the exit of the mass spectrometer switched off". How much signal do you get when the pump is on? What causes the difference?
Authors : The ion pump is responsible for creating the equivalent of about 50 counts per second. These are probably caused by either electrons or X-rays emitted by the pump and not stopped by the pump geometry.